Prescribed Performance Image Based Visual Servoing under Field of View Constraints

Shahab Heshmati-alamdari, Charalampos P. Bechlioulis, Minas V. Liarokapis and Kostas J. Kyriakopoulos

***Abstract*— In this paper, we propose a novel image based visual servoing scheme that imposes prescribed transient and steady state response on the image feature coordinate errors and satisfies the visibility constraints that inherently arise owing to the limited field of view (FOV) of cameras. Visualizing the aforementioned performance specifications as error bounds, the key idea is to provide an error transformation that converts the original constrained problem into an equivalent unconstrained one, the stabilization of which proves sufficient to achieve prescribed performance guarantees and satisfy the inherent visibility constraints. The performance of the developed scheme is a priori and explicitly imposed by certain designer-specified performance functions, and is fully decoupled by the control gains selection, thus simplifying the control design. Moreover, its computational complexity proves significantly low. It is actually a static scheme involving very few and simple calculations to output the control signal, which enables easily its implementation on fast embedded control platforms. Finally, real-time experiments using an eye-in-hand robotic system verify the theoretical findings.**

I. Introduction

Over the last decades, visual servoing has gained a lot of research interest in motion control systems. In general, it employs the visual information of a camera as feedback to determine the required control signal. Structurally, visual servoing can be classified as: (i) Position-Based Visual Servoing (PBVS), where the visual features extracted from the image are used to estimate the $3D$ pose of the robot wrt the target; (ii) Image-Based Visual Servoing (IBVS), where the control inputs are determined directly on the $2D$ image plane based on the error of the image features between the current and desired images, and (iii) Hybrid Visual Servoing, where $3D$ PBVS is combined with $2D$ IBVS [1]–[3]. In this paper, the IBVS scheme is considered, as it is more efficient than the other two, owing to its inherent robustness against camera calibration imperfections.

Since visual servoing is mainly based on visual information extracted from the position of the features of interest on the camera image, a significant issue that reasonably raises concerns the satisfaction of certain hard visibility constraints, imposed by the fact that the features of interest should constantly lie in the camera FOV during the motion of the camera [4]. Although dealing with hard constraints is very challenging, various methods have been developed towards this direction. More specifically, in [5] and [6] the FOV constraints are studied under a Model Predictive Control framework. Furthermore, in [7]–[10] path planning of the camera motion in 3D space and subsequently projection onto the image plane are adopted to calculate a camera motion that does not violate the FOV constraints. Unfortunately, the aforementioned strategies rely heavily on the knowledge of 3D reconstruction and camera calibration parameters. Furthermore, their applicability in fast real-time implementations becomes questionable, owing to the computationally demanding optimization processing.

Another important issue associated with IBVS schemes concerns the transient and steady state response of the closed loop system. Unfortunately, apart from the [11], in which the authors assume some bounds on task error, there is no systematic procedure to accurately impose predefined transient and steady state performance specifications. Towards this direction, the common practice in conventional IBVS schemes is to tune appropriately the control gains without, however, any a priori guarantees for the achieved performance.

In this work, motivated by [12], we propose a novel IBVS scheme, capable of guaranteeing prescribed transient and steady state performance as well as satisfaction of the FOV constraints. Visualizing the performance specifications and the FOV constraints as error bounds, the key idea is to provide an error transformation that converts the original constrained model into an equivalent unconstrained one. It is then proven that stabilizing the unconstrained model is sufficient to achieve prescribed performance guarantees and satisfy the FOV constraints. Moreover, the performance of the developed scheme is a priori and explicitly imposed by certain designer-specified performance functions, and is fully decoupled by the control gains selection. In that respect, the selection of the control gains is only confined to adopting those values that lead to reasonable control effort, thus simplifying further the control design. Finally, the computational complexity of the proposed scheme proves considerably low (i.e., it is a static scheme involving very few and simple calculations to output the control signal), which makes implementation on fast embedded control platforms straightforward.

The paper is organized as follows. The model and some preliminary results, necessary in the subsequent analysis, are given in Section II. The main results are provided in Section III. The Section IV presents experimental results. Finally, we conclude in Section V.

The authors are with the Control Systems Lab, School of Mechanical Engineering, National Technical University of Athens, 9 Heroon Polytechniou Street, Zografou 15780, Greece {shahab,chmpechl,mliaro,kkyria@mail.ntua.gr}.

This work was supported by the EU funded project PANDORA: Persistent Autonomy through learNing, aDaptation, Observation and ReplAnning, FP7-288273, 2012-2014.

II. Model Description and Preliminaries

In this section, the mathematical formulation of the image based visual servoing problem is presented for a pinhole camera model. Let $[X_c, Y_c, Z_c]^\top$ be the axes of the camera frame $\mathcal{C}$ attached at the center of the camera O_c. The coordinates of the image frame $\mathcal{I}$ are given by $[u, v]^\top$ with O_I denoting the center of the image, as depicted in Fig. 1. Notice that the Z_c axis of the camera frame is perpendicular to the image plane transversing O_I. In this way, given a set of

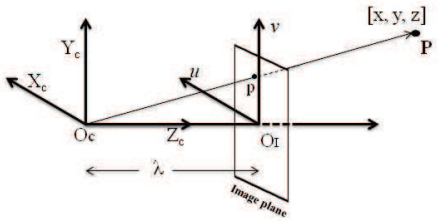

Fig. 1: The geometric model of a pinhole camera.

n fixed 3D points $P_i = [x_i, y_i, z_i]^\top$, $i = 1, \ldots, n$ expressed in the camera frame, the corresponding 2D image feature $s_i = [u_i, v_i]^\top$, $i = 1, \ldots, n$ are given as follows [13]:

$$s_i = \begin{bmatrix} u_i \\ v_i \end{bmatrix} = \frac{\lambda}{z_i} \begin{bmatrix} x_i \\ y_i \end{bmatrix} \tag{1}$$

where λ is the focal length of the camera (see Fig.1). Thus, the effect of the camera motion on the feature coordinates at the image plane is given by:

$$\dot{s}_i = L_i(z_i, s_i)V,\ i = 1, \ldots, n \tag{2}$$

where:

$$L_i(z_i, s_i) = \begin{bmatrix} -\frac{\lambda}{z_i} & 0 & \frac{\lambda u_i}{z_i} & u_i v_i & -(1+u_i^2) & v_i \\ 0 & -\frac{\lambda}{z_i} & \frac{\lambda v_i}{z_i} & (1+v_i^2) & -u_i v_i & -u_i \end{bmatrix}$$

is the interaction matrix [13], and

$$V = \begin{bmatrix} T \\ \Omega \end{bmatrix} = [T_x, T_y, T_z, \omega_x, \omega_y, \omega_z]^\top$$

denotes the translational and angular velocities of the camera. Let us also define the overall image feature vector $s = \left[s_1^\top, \cdots, s_n^\top\right]^\top \in \mathcal{R}^{2n}$, the time derivative of which is given by:

$$\dot{s} = L(z, s)V \tag{3}$$

where $L(z, s) = \left[L_1^\top(z_1, s_1), \cdots, L_n^\top(z_n, s_n)\right]^\top$ is the overall interaction matrix and $z = [z_1, \ldots, z_n]^\top$. Finally, owing to the limited field of view of the camera, the image coordinates are subject to the following visibility constraints:

$$u_{\min} \leq u_i \leq u_{\max},\ i = 1, \ldots, n \tag{4a}$$

$$v_{\min} \leq v_i \leq v_{\max},\ i = 1, \ldots, n \tag{4b}$$

where $u_{\min}$, $v_{\min}$ and $u_{\max}$, $v_{\max}$ are the lower and upper bounds (in pixels) of the image plane coordinates u, v respectively. Thus, ensuring that the feature coordinates do not violate the aforementioned visibility constraints is a significant issue raised when designing IBVS schemes.

A. Dynamical Systems

Consider the initial value problem:

$$\dot{\psi} = H(t, \psi), \quad \psi(0) = \psi^0 \in \Omega_\psi \tag{5}$$

with $H : \mathcal{R}_+ \times \Omega_\psi \to \mathcal{R}^m$ where $\Omega_\psi \subset \mathcal{R}^m$ is a non-empty open set.

Definition 1: [14] A solution $\psi(t)$ of the initial value problem (5) is maximal if it has no proper right extension that is also a solution of (5)

Theorem 1: [14] Consider the initial value problem (5). Assume that $H(t, \psi)$ is : a) locally Lipschitz on ψ for almost all $t \in \mathcal{R}_+$, b) piecewise continuous on t for each fixed $\psi \in \Omega_\psi$ and c) locally integrable on t for each fixed $\psi \in \Omega_\psi$. Then there exists a maximal solution $\psi(t)$ of (5) on the time interval $[0,\ \tau_{max})$ with $\tau_{max} > 0$ such that $\psi(t) \in \Omega_\psi,\ \forall t \in [0,\ \tau_{max})$.

Proposition 1: [14] Assume that the hypotheses of the Theorem 1 hold. For a maximal solution $\psi(t)$ on the time interval $[0,\ \tau_{max})$ with $\tau_{max} < \infty$ and for any compact set $\Omega'_\psi \subset \Omega_\psi$ there exists a time instant $t' \in [0,\ \tau_{max})$ such that $\psi(t') \notin \Omega'_\psi$.

III. IBVS with Prescribed Performance

Let us initially define the image feature errors:

$$e_i^u = u_i - u_i^\star,\ i = 1, \ldots, n \tag{6a}$$

$$e_i^v = v_i - v_i^\star,\ i = 1, \ldots, n \tag{6b}$$

where $u_i^\star$, $v_i^\star$ denote the corresponding desired feature values, as well as the overall error vector:

$$e = \left[e_1^u, e_1^v, \ldots, e_n^u, e_n^v\right]^\top.$$

The control design is based on the prescribed performance notion that was proposed to design robust state feedback controllers, for various classes of nonlinear systems [12], [15] and [16]. In this work, prescribed performance control will be adopted in order to achieve: i) predefined transient and steady state response as well as ii) maintenance of the features of interest in the camera field of view. More specifically, prescribed performance is achieved when the errors $e_i^u(t)$, $e_i^v(t)$, $i = 1, \ldots, n$ evolve strictly within a predefined region that is bounded by absolutely decaying functions of time, called performance functions. The mathematical expression of prescribed performance is given, for all $t \geq 0$, by the following inequalities:

$$-\underline{M}_i^u\ \underline{\rho}_i^u(t) < e_i^u(t) < \bar{M}_i^u\ \bar{\rho}_i^u(t) \tag{7a}$$

$$-\underline{M}_i^v\ \underline{\rho}_i^v(t) < e_i^v(t) < \bar{M}_i^v\ \bar{\rho}_i^v(t) \tag{7b}$$

for $i = 1, \ldots, n$, where:

$$\underline{\rho}_i^u(t) = (1 - \frac{\rho_\infty}{\underline{M}_i^u})\exp(-lt) + (\frac{\rho_\infty}{\underline{M}_i^u}) \tag{8a}$$

$$\bar{\rho}_i^u(t) = (1 - \frac{\rho_\infty}{\bar{M}_i^u})\exp(-lt) + (\frac{\rho_\infty}{\bar{M}_i^u}) \tag{8b}$$

$$\underline{\rho}_i^v(t) = (1 - \frac{\rho_\infty}{\underline{M}_i^v})\exp(-lt) + (\frac{\rho_\infty}{\underline{M}_i^v}) \tag{8c}$$

$$\bar{\rho}_i^v(t) = (1 - \frac{\rho_\infty}{\bar{M}_i^v})\exp(-lt) + (\frac{\rho_\infty}{\bar{M}_i^v}) \tag{8d}$$

are designer-specified smooth, bounded, strictly positive and decreasing functions of time, selected appropriately to impose the desired transient and steady state response. More specifically, their decreasing rate, which is affected by the constant l, introduces a lower bound on the speed of the convergence of $e_i^u(t)$, $e_i^v(t)$, $i = 1, \ldots, n$. Furthermore, the constant $\rho_\infty > 0$ can be set arbitrarily small, thus achieving practical convergence of $e_i^u(t)$, $e_i^v(t)$, $i = 1, \ldots, n$ to zero. Additionally, the constants $\underline{M}_i^u$, $\bar{M}_i^u$, $\underline{M}_i^v$, $\bar{M}_i^v$, $i = 1, \ldots, n$ are selected appropriately to guarantee that the features remain inside the camera field of view if (7a)-(7b) are satisfied. Under the assumption that the features initially lie in the camera field of view (i.e., $u_{min} < u_i(0) < u_{max}$ and $v_{min} < v_i(0) < v_{max}$, $i = 1, \ldots, n$), we select the parameters $\underline{M}_i^u$, $\bar{M}_i^u$, $\underline{M}_i^v$, $\bar{M}_i^v$ as:

$$\underline{M}_i^u = u_i^* - u_{min}, \qquad \bar{M}_i^u = u_{max} - u_i^* \tag{9a}$$
$$\underline{M}_i^v = v_i^* - v_{min}, \qquad \bar{M}_i^v = v_{max} - v_i^* \tag{9b}$$

for $i = 1, \ldots, n$. Apparently, the aforementioned selection initially ensures that:

$$-\underline{M}_i^u \ \underline{\rho}_i^u(0) < e_i^u(0) < \bar{M}_i^u \ \bar{\rho}_i^u(0) \tag{10a}$$
$$-\underline{M}_i^v \ \underline{\rho}_i^v(0) < e_i^v(0) < \bar{M}_i^v \ \bar{\rho}_i^v(0) \tag{10b}$$

for $i = 1, \ldots, n$. Moreover, guaranteeing (7a)-(7b) for all $t \geq 0$ and owing to the decreasing property of $\underline{\rho}_i^u(t)$, $\bar{\rho}_i^u(t)$, $\underline{\rho}_i^v(t)$, $\bar{\rho}_i^v(t)$, $i = 1, \ldots, n$, we obtain:

$$-\underline{M}_i^u < e_i^u(t) < \bar{M}_i^u, \ i = 1, \ldots, n \tag{11a}$$
$$-\underline{M}_i^v < e_i^v(t) < \bar{M}_i^v, \ i = 1, \ldots, n \tag{11b}$$

which further leads via (9a)-(9b) to the satisfaction of the FOV constraints (4a)-(4b) for all $t \geq 0$. The aforementioned statements are clearly illustrated in Fig. 2 for two exponentially decreasing performance functions $\underline{M}_i^v \underline{\rho}_i^v(t)$, $\bar{M}_i^v \bar{\rho}_i^v(t)$ with $\underline{M}_i^v$, $\bar{M}_i^v$ satisfying (9a)-(9b) and ρ_∞, l appropriately selected positive constants imposing the desired transient and steady state response.

Theorem 2: Consider system (3), the FOV constraints (4a)-(4b) as well as the image feature errors (6a)-(6b), and design appropriately the performance functions according to (9a)-(9b) and the desired transient and steady state performance specifications. The control law:

$$V(s,t) = -kL^+E \text{ with } k > 0 \tag{12}$$

where L^+ is the pseudo-inverse of the interaction matrix, and:

$$E = \begin{bmatrix} E_u^1 \\ E_v^1 \\ \vdots \\ E_u^n \\ E_v^n \end{bmatrix} := \begin{bmatrix} \ln\left(\frac{1+\xi_1^u}{1-\xi_1^u} \cdot \frac{\bar{M}_1^u \bar{\rho}_1^u(t)}{\underline{M}_1^u \underline{\rho}_1^u(t)}\right) \\ \ln\left(\frac{1+\xi_1^v}{1-\xi_1^v} \cdot \frac{\bar{M}_1^v \bar{\rho}_1^v(t)}{\underline{M}_1^v \underline{\rho}_1^v(t)}\right) \\ \vdots \\ \ln\left(\frac{1+\xi_n^u}{1-\xi_n^u} \cdot \frac{\bar{M}_n^u \bar{\rho}_n^u(t)}{\underline{M}_n^u \underline{\rho}_n^u(t)}\right) \\ \ln\left(\frac{1+\xi_n^v}{1-\xi_n^v} \cdot \frac{\bar{M}_1^v \bar{\rho}_n^v(t)}{\underline{M}_n^v \underline{\rho}_n^v(t)}\right) \end{bmatrix} \tag{13}$$

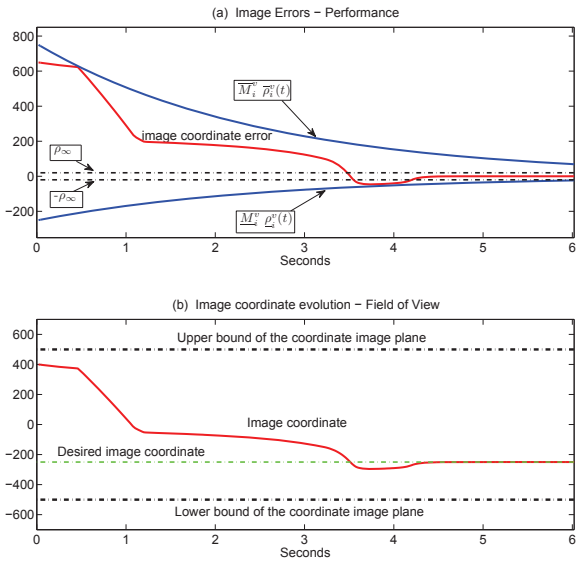

Fig. 2: (a) Graphical illustration of prescribed performance (7b). (b) Graphical illustration of (4b).

with the normalized feature errors:

$$\xi_i^u = \frac{e_i^u - \frac{\bar{M}_i^u \bar{\rho}_i^u(t) - \underline{M}_i^u \underline{\rho}_i^u(t)}{2}}{\frac{\bar{M}_i^u \bar{\rho}_i^u(t) + \underline{M}_i^u \underline{\rho}_i^u(t)}{2}}, \ i = 1, \ldots, n$$
$$\xi_i^v = \frac{e_i^v - \frac{\bar{M}_1^v \bar{\rho}_i^v(t) - \underline{M}_i^v \underline{\rho}_i^v(t)}{2}}{\frac{\bar{M}_1^v \bar{\rho}_i^v(t) + \underline{M}_i^v \underline{\rho}_i^v(t)}{2}}, \ i = 1, \ldots, n$$

guarantees local practically asymptotic stabilization of the feature errors as dictated by (7a)-(7b) and thus prescribed transient and steady state performance without violating the FOV constraints.

Proof: To prove our concept, we first define the normalized error vector:

$$\xi = [\xi_1^u, \xi_1^v, \ldots, \xi_n^u, \xi_n^v]^\top.$$

Differentiating the normalized feature errors wrt time and substituting (3), (12) and (13), the closed loop dynamical system of the ξ may be written as:

$$\dot{\xi} = h(t, \xi) \tag{14}$$

where the function $h(t, \xi)$ includes all terms found at the right hand side after the differentiation of ξ. Let us also define the open set $\Omega_\xi = (-1, 1)^{2n}$. In what follows, we proceed in two phases. First, the existence of a maximal solution $\xi(t)$ of (14) over the set Ω_ξ for a time interval $[0, \ \tau_{max})$ (i.e., $\xi(t) \in \Omega_\xi, \ \forall t \in [0, \ \tau_{max})$) is ensured. Then, we prove that the proposed control scheme (12) guarantees, for all $t \in [0, \ \tau_{max})$: a) the boundedness of all closed loop signals as well as that b) $\xi(t)$ remains strictly within a compact subset of Ω_ξ, which leads by contradiction to $\tau_{max} = \infty$ and consequently to the satisfaction of (7a)-(7b) which completes the proof.

Phase 1: The set Ω_ξ is nonempty and open. Moreover, ensuring (10a)-(10b) leads to $-1 < \xi_i^u(0) < 1$ and $-1 <$

$\xi_i^v(0) < 1,\ i = 1, \ldots, n$. Thus we conclude that $\xi(0) \in \Omega_\xi$. Additionally, $h(t, \xi)$, is continuous on t and locally Lipschitz on ξ over the set Ω_ξ. Therefore, the hypotheses of Theorem 1 stated in Subsection II-A hold and the existence of a maximal solution $\xi(t)$ of (14) on a time interval $[0,\ \tau_{max})$ such that $\xi(t) \in \Omega_\xi,\ \forall t \in [0,\ \tau_{max})$ is ensured.

Phase 2: We have proven in Phase 1 that $\xi(t) \in \Omega_x,\ \forall t \in [0,\ \tau_{max})$ and more specifically that:

$$\xi_i^u(t) \in (-1, 1) \text{ and } \xi_i^v(t) \in (-1, 1),\ i = 1, \ldots, n$$

for all $t \in [0,\ \tau_{max})$. Thus, the transformed errors E_i^u, E_i^v, $i = 1, \ldots, n$, as defined in (13), are well defined for all $t \in [0,\ \tau_{max})$ and moreover, it can be easily verified that $e_i^u \to 0$ implies $E_i^u \to \ln(1) = 0$ and $e_i^v \to 0$ implies $E_i^v \to \ln(1) = 0$, $i = 1, \ldots, n$. To proceed, we define, based on the transformed errors (13), the following task function [17]:

$$\varepsilon = L^+ E.$$

Contrary to [17], where L^+ is assumed constant, in this work we consider the general case where L^+ is state dependent. Thus, the time derivative of the task function becomes:

$$\begin{aligned}\dot{\varepsilon} &= \frac{dL^+}{dt}E + L^+\dot{E} \\ &= \frac{dL^+}{dt}E + L^+\Big[\frac{\partial E}{\partial \xi}\big(\frac{\partial \xi}{\partial e}LV + \frac{\partial \xi}{\partial t}\big) + \frac{\partial E}{\partial t}\Big] \end{aligned} \tag{15}$$

Following [18], we also obtain:

$$\frac{dL^+}{dt}E = O(e, t)V$$

where $O(e, t)$ is a 6×6 matrix satisfying $O(e, t)|_{e=0} = \mathbf{0}$, $\forall t \geq 0$. Hence, (15) becomes:

$$\dot{\varepsilon} = \Big[O(e, t) + L^+\big(\frac{\partial E}{\partial \xi}\frac{\partial \xi}{\partial e}\big)L\Big]V + L^+\Big[\frac{\partial E}{\partial \xi}\frac{\partial \xi}{\partial t} + \frac{\partial E}{\partial t}\Big]$$

and substituting the control law:

$$V = -kL^+E = -k\varepsilon$$

we get:

$$\dot{\varepsilon} = -k\Big[O(e, t) + L^+\big(\frac{\partial E}{\partial \xi}\frac{\partial \xi}{\partial e}\big)L\Big]\varepsilon + L^+\Big[\frac{\partial E}{\partial \xi}\cdot\frac{\partial \xi}{\partial t} + \frac{\partial E}{\partial t}\Big]. \tag{16}$$

Finally, linearizing (16) for $e = 0$, we obtain similarly to [18]:

$$\dot{\varepsilon} = -kA(t)\varepsilon + B(t),$$

where:

$$A(t) = L^+\big(\frac{\partial E}{\partial \xi}\frac{\partial \xi}{\partial e}\big)L\Big|_{e=0} \tag{17a}$$

$$B(t) = L^+\Big(\frac{\partial E}{\partial \xi}\frac{\partial \xi}{\partial t} + \frac{\partial E}{\partial t}\Big)\Big|_{e=0}. \tag{17b}$$

Notice also that by construction $\frac{\partial E}{\partial \xi}\frac{\partial \xi}{\partial e}$ is a diagonal positive definite matrix. Thus, following similar arguments with the proof of Proposition 1 in [19], we conclude that $A(t) = L^+\big(\frac{\partial E}{\partial \xi}\frac{\partial \xi}{\partial e}\big)L\Big|_{e=0}$ is also positive definite. Moreover, it can be easily verified that the vector $B(t)$ is bounded for all $t \geq 0$ (i.e, there exists a positive constant $\bar{B}$ such that $||B(t)|| \leq \bar{B},\ \forall t \leq 0$). Hence, we conclude that $\varepsilon(t) \leq \bar{\varepsilon} = \max\Big\{||\varepsilon(0)||,\ \frac{\lambda_{\min}(A)\bar{B}}{k}\Big\}$ for all $\forall t \in [0,\ \tau_{max})$ in a neighborhood of $e = 0$. Moreover, in a neighborhood of $e = 0$, we have $||\varepsilon|| = ||L^+E|| \neq 0$ if $e \neq 0$ or equivalently if $E \neq 0$ [20]. Hence, there exists $\delta > 0$ such that $||\varepsilon|| = ||L^+E|| \geq \delta||E||$, from which we obtain:

$$||E(t)|| \leq \frac{\bar{\varepsilon}}{\delta},\ \forall t \in [0,\ \tau_{max}). \tag{18}$$

In this way, taking the inverse logarithmic function in (13), we get:

$$\begin{aligned} -1 < \underline{\xi}_i^u < \xi_i^u(t) < \bar{\xi}_i^u < 1,\ i = 1, \ldots, n \\ -1 < \underline{\xi}_i^v < \xi_i^v(t) < \bar{\xi}_i^v < 1,\ i = 1, \ldots, n \end{aligned} \tag{19}$$

for all $t \in [0,\ \tau_{max})$, where:

$$\begin{aligned} \underline{\xi}_i^u &= \frac{1 - \max\Big\{1, \frac{\bar{M}_i^u}{\underline{M}_i^u}\Big\}\exp(\frac{\bar{\varepsilon}}{\delta})}{1 + \max\Big\{1, \frac{\bar{M}_i^u}{\underline{M}_i^u}\Big\}\exp(\frac{\bar{\varepsilon}}{\delta})}, \\ \bar{\xi}_i^u &= \frac{\max\Big\{1, \frac{\underline{M}_i^u}{\bar{M}_i^u}\Big\}\exp(\frac{\bar{\varepsilon}}{\delta}) - 1}{\max\Big\{1, \frac{\underline{M}_i^u}{\bar{M}_i^u}\Big\}\exp(\frac{\bar{\varepsilon}}{\delta}) + 1} \\ \underline{\xi}_i^v &= \frac{1 - \max\Big\{1, \frac{\bar{M}_i^v}{\underline{M}_i^v}\Big\}\exp(\frac{\bar{\varepsilon}}{\delta})}{1 + \max\Big\{1, \frac{\bar{M}_i^v}{\underline{M}_i^v}\Big\}\exp(\frac{\bar{\varepsilon}}{\delta})}, \\ \bar{\xi}_i^v &= \frac{\max\Big\{1, \frac{\underline{M}_i^v}{\bar{M}_i^v}\Big\}\exp(\frac{\bar{\varepsilon}}{\delta}) - 1}{\max\Big\{1, \frac{\underline{M}_i^v}{\bar{M}_i^v}\Big\}\exp(\frac{\bar{\varepsilon}}{\delta}) + 1}. \end{aligned}$$

Finally, it can be easily proven from (13) that the control input (12) remains also bounded for all $t \in [0,\ \tau_{max})$.

Up to this point, what remains to be shown is that τ_{max} can be extended to ∞. Notice by (19) that $\xi(t) \in \Omega'_\xi,\ \forall t \in [0, \tau_{max})$, where the set:

$$\Omega'_\xi = \big[\underline{\xi}_1^u, \bar{\xi}_1^u\big] \times \big[\underline{\xi}_1^v, \bar{\xi}_1^v\big] \times \cdots \times \big[\underline{\xi}_n^u, \bar{\xi}_n^u\big] \times \big[\underline{\xi}_n^v, \bar{\xi}_n^v\big]$$

is a nonempty and compact subset of Ω_ξ. Hence, assuming $\tau_{max} < \infty$ and since $\Omega'_\xi \subset \Omega_\xi$, Proposition 1 in Subsection II-A dictates the existence of a time instant $t' \in [0, \tau_{max})$ such that $\xi(t') \notin \Omega'_\xi$, which is a clear contradiction. Therefore, $\tau_{max} = \infty$. As a result, all closed loop signals remain bounded and moreover $\xi(t) \in \Omega'_\xi \subset \Omega_\xi,\ \forall t \geq 0$. Finally, from (19) we conclude the satisfaction of (7a)-(7b) for all $t \geq 0$ and consequently guaranteed prescribed performance without violating the FOV constraints, which completes the proof.

■

Remark 1: From the aforementioned proof, it can be deduced that the proposed IBVS scheme achieves its goals (i.e., prescribed performance and FOV constraints) without residing on the need of rendering $\frac{\bar{\varepsilon}}{\delta}$ arbitrarily small (see (18)), by adopting an extreme value for the control gain k. More specifically, notice that (19) and consequently (7a)-(7b), which encapsulate the prescribed performance notion and the FOV constraints, hold no matter how large the

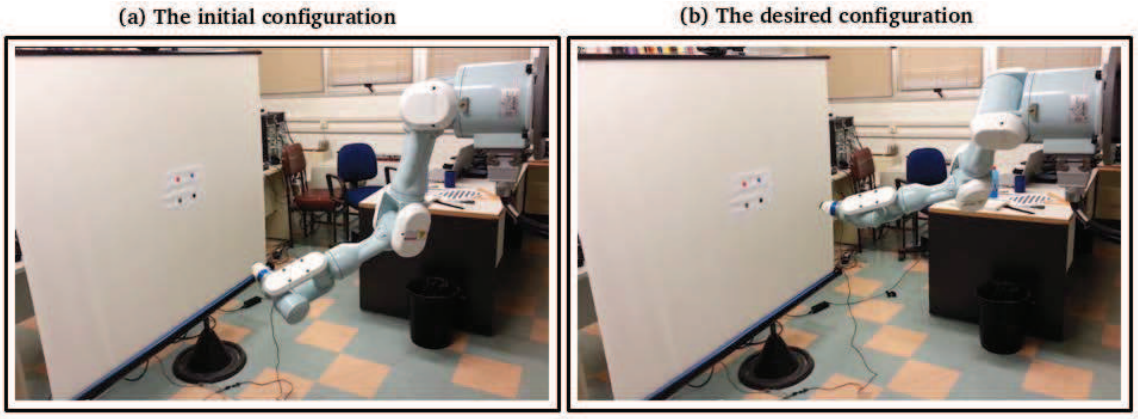

Fig. 3: The experimental setup comprises of a USB camera attached at the end effector of the Mitsubishi PA-10 robot arm observing the planar target. (a) The initial camera pose. (b) The desired camera pose.

finite bound $\frac{\bar{\varepsilon}}{\delta}$ is. Thus, contrary to what is the common practice in the related literature (i.e., the control gains are tuned towards satisfying a desired performance, nonetheless without any a priori guarantees), the actual performance of the proposed IBVS scheme is solely determined by the performance functions $\underline{M}_i^u \underline{\rho}_i^u(t)$, $\bar{M}_i^u \bar{\rho}_i^u(t)$, $\underline{M}_i^v \underline{\rho}_i^v(t)$, $\bar{M}_i^v \bar{\rho}_i^v(t)$, $i = 1, \ldots, n$. Hence, the selection of the control gain k is significantly simplified to adopting those values that lead to reasonable control effort. Finally, the computational complexity of the proposed scheme proves considerably low. It is actually a static scheme involving very few simple calculations to output the control signal, which enables easily its implementation on fast embedded control platforms.

IV. Experimental Results

To validate the theoretical results and verify the efficiency of the proposed PP-IBVS scheme, an experiment was conducted using a Mitsubishi PA-10 7 DoF robotic manipulator equipped with a calibrated perspective USB camera observing a planar target, as depicted in Fig. 3. The target consists of four colored circles the center of which denotes the feature image coordinates. The desired pose of the target wrt the camera frame is $p^* = [0, 0, 0.4, 0, 0, 0]$. Thus, the desired feature coordinates, which were extracted by an image captured at the aforementioned desired pose of the camera, were $s^* = [92.5, -92.5, -92.5, -92.5, 92.5, 92.5, -92.0, 92.0]$. Finally, the initial pose of the target wrt the camera frame and the initial feature coordinates were $p(0) = [-0.229, 0.11, 0.518, 0.375, 0.324, -0.497]$ and $s(0) = [-99.0, -116.5, -197.0, -52, -25.5, -12.5, -123.5, 42.5]$ respectively. As mentioned in the previous section the initial value of the upper and lower performance functions for each image feature coordinate is chosen such that all features are retained within the camera FOV. More specifically, for the following upper and lower bounds of image plane of the considered camera:

$$u_{\max} = 319 \quad u_{\min} = -319$$
$$v_{\max} = 239 \quad v_{\min} = -239$$

TABLE I

Image Feature	Coordinate	$\bar{M}_i$	$\underline{M}_i$
Feature 1	**u**	226.5	-411.5
	v	331.5	-145.5
Feature 2	**u**	411.5	-226.5
	v	331.5	-146.5
Feature 3	**u**	226.5	-411.5
	v	146.5	-331.5
Feature 4	**u**	411.0	-227.0
	v	147.0	-331.0

the parameters $\bar{M}_i^u$, $\underline{M}_i$, $i = 1, \ldots, 4$ are shown in Table I. Furthermore, the performance parameter ρ_∞ was selected equal to 5 pixels. Thus, ultimately the center of each feature will be restrained within a square of 10 pixels edge around the desired position in the image plane. Finally, the decreasing rate l was chosen equal to $l = 0.45$.

As it was expected, the feature coordinate errors were retained in the corresponding performance areas (see Fig. 4) and consequently the features were constrained within the camera FOV as presented in Fig. 5. Finally, the required control input signals are illustrated in Fig. 6.

V. Conclusions

This work presents a novel image based visual servoing scheme that achieves prescribed transient as well as steady state performance on the image feature coordinate errors and satisfies the camera field of view constraints. The developed controller exhibits the following important characteristics. First, it is of low complexity and thus it can be used effectively in fast embedded control systems. Additionally, the a priori guaranteed performance, by certain designer-specified functions, simplifies significantly the selection of the controller parameters. Gain tuning is only confined to achieving reasonable control effort. Finally, future research

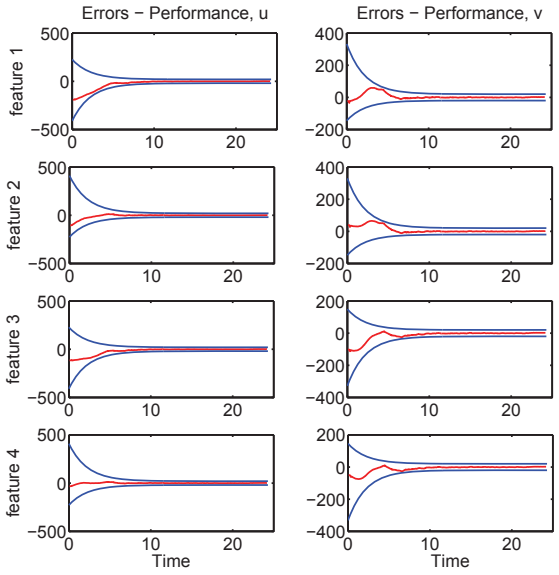

Fig. 4: The evolution of the feature coordinate errors along with the corresponding imposed performance bounds.

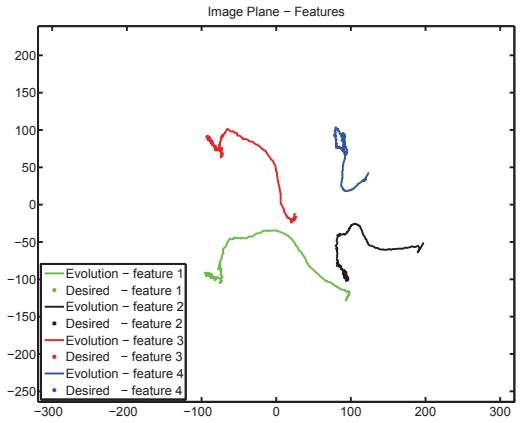

Fig. 5: The evolution of the features on the image plane. The desired position of the features on the image plane is denoted by $*$.

efforts will be devoted towards addressing parametric uncertainties on the camera model.

REFERENCES

[1] F. Chaumette and S. Hutchinson, "Visual servo control. i. basic approaches," *IEEE Robotics and Automation Magazine*, vol. 13, no. 4, pp. 82–90, 2006.

[2] ——, "Visual servo control, part ii: Advanced approaches," *IEEE Robotics and Automation Magazine*, vol. 14, no. 1, pp. 109–118, 2007.

[3] E. Malis, F. Chaumette, and S. Boudet, "2-1/2-d visual servoing," *IEEE Transactions on Robotics and Automation*, vol. 15, no. 2, pp. 238–250, 1999.

[4] F. Chaumette, "Potential problems of stability and convergence in image-based and position-based visual servoing," in *The confluence of vision and control*. Springer London, 1998, vol. 237, pp. 66–78.

[5] G. Allibert, E. Courtial, and F. Chaumette, "Predictive control for constrained image-based visual servoing," *IEEE Transactions on Robotics*, vol. 26, no. 5, pp. 933–939, 2010.

[6] S. Heshmati-alamdari, G. K. Karavas, A. Eqtami, M. Drossakis, and K. J. Kyriakopoulos, "Robustness analysis of model predictive control for constrained image-based visual servoing," in *IEEE International Conference on Robotics and Automation (ICRA)*, 2014.

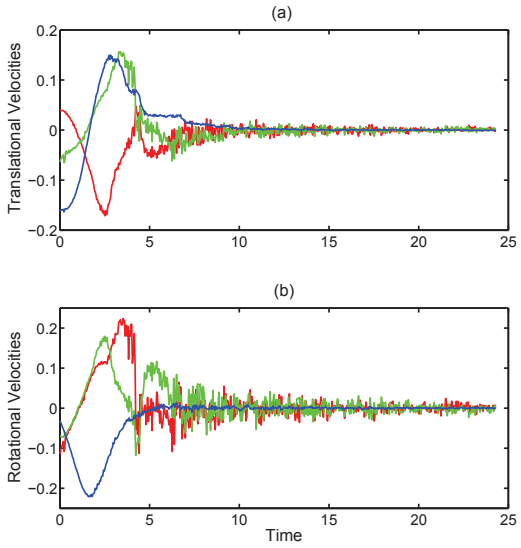

Fig. 6: The control input signals. (a) The translational velocities. (b) The rotational velocities.

[7] G. Chesi, "Visual servoing path planning via homogeneous forms and lmi optimizations," *IEEE Transactions on Robotics*, vol. 25, no. 2, pp. 281–291, 2009.

[8] M. Kazemi, K. Gupta, and M. Mehrandezh, "Global path planning for robust visual servoing in complex environments," in *IEEE International Conference on Robotics and Automation (ICRA)*, 2009, pp. 1726–1732.

[9] ——, "Randomized kinodynamic planning for robust visual servoing," *IEEE Transactions on Robotics*, vol. 29, no. 5, pp. 1197–1211, 2013.

[10] Y. Mezouar and F. Chaumette, "Path planning for robust image-based control," *IEEE Transactions on Robotics and Automation*, vol. 18, no. 4, pp. 534–549, 2002.

[11] G. Morel, P. Zanne, and F. Plestan, "Robust visual servoing: Bounding the task function tracking errors," *IEEE Transactions on Control Systems Technology*, vol. 13, no. 6, pp. 998–1009, 2005.

[12] C. P. Bechlioulis and G. A. Rovithakis, "Robust adaptive control of feedback linearizable mimo nonlinear systems with prescribed performance," *IEEE Transactions on Automatic Control*, vol. 53, no. 9, pp. 2090–2099, 2008.

[13] S. Hutchinson, G. Hager, and P. Corke, "A tutorial on visual servo control," *IEEE Transactions on Robotics and Automation*, vol. 12, no. 5, pp. 651–670, 1996.

[14] E. D. Sontag, *Mathematical Control Theory*. London, U.K.: Springer, 1998.

[15] C. P. Bechlioulis and G. A. Rovithakis, "Adaptive control with guaranteed transient and steady state tracking error bounds for strict feedback systems," *Automatica*, vol. 45, no. 2, pp. 532–538, 2009.

[16] ——, "Prescribed performance adaptive control for multi-input multi-output affine in the control nonlinear systems," *IEEE Transactions on Automatic Control*, vol. 55, no. 5, pp. 1220–1226, 2010.

[17] B. Espiau, F. Chaumette, and P. Rives, "A new approach to visual servoing in robotics," *IEEE Transactions on Robotics and Automation*, vol. 8, no. 3, pp. 313–326, 1992.

[18] E. Malis and P. Rives, "Robustness of image-based visual servoing with respect to depth distribution errors," in *IEEE International Conference on Robotics and Automation (ICRA)*, 2003, pp. 1056–1061.

[19] E. Malis, "Visual servoing invariant to changes in camera-intrinsic parameters," *IEEE Transactions on Robotics and Automation*, vol. 20, no. 1, pp. 72–81, 2004.

[20] E. Malis and F. Chaumette, "Theoretical improvements in the stability analysis of a new class of model-free visual servoing methods," *IEEE Transactions on Robotics and Automation*, vol. 18, no. 2, pp. 176–186, 2002.